3-D Elastic Modeling with Surface Topography by a Chebychev Spectral Method

ST3.4

Ekkehart Tessmer, Univ. Hamburg (UH), Germany; and Dan Kosloff, Tel Aviv Univ., Israel and UH*

SUMMARY

A 3-dimensional numerical modeling scheme which accounts for surface topography is presented. The method is based on spectral derivative operators. Spatial differencing in the horizontal directions is performed by the Fourier method, whereas vertical derivatives are carried out by a Chebyshev method which allows for the incorporation of boundary conditions. The implementation of surface topography is done by mapping a rectangular grid onto a curved grid.

The study of near surface effects of seismic wave propagation in the presence of surface topography is important since non-ray effects such as diffractions and scattering at rough surfaces must be considered as wave phenomena.

The modeling algorithm presented here can serve as a tool for understanding these phenomena. All wave types are included in the solution since the full wave field is computed.

A 3D modeling example of a half space with a trench at the surface is given.

INTRODUCTION

Surface topography and the weathered zone have great influence on seismic reflection surveys. In case of mild topography and low velocity heterogeneity the effects of topography and the weathering zone can be removed by static corrections. However, in case of a rough surface and a heterogeneous weathering layer the seismograms are contaminated by diffractions and the behavior of the ground roll becomes more difficult.

Various direct methods can be applied to the surface topography problem in conjunction with high material heterogeneity, e.g. finite differences and finite elements, where the latter method is more flexible. However, these methods are usually of low order.

It is difficult to incorporate boundary conditions into high order finite difference or spectral methods. An exception is the Chebyshev spectral method (Kosloff et al., 1990) which is of high accuracy. This method can handle the free surface boundary conditions correctly by using the concept of characteristic variables (Gottlieb et al., 1982).

EQUATION OF MOTION

The equations of motion for a three-dimensional isotopic medium are given by

$$\varrho \frac{\partial^2 u_i}{\partial t^2} = \frac{\partial \sigma_{ij}}{\partial x_j} + f_i, \quad i = 1,2,3 \tag{1}$$

where x_j are Cartesian coordinates, σ_{ij} are the stress components, u_i are the displacements, ϱ is the density and f_i denotes the body forces. The stress-strain relations for an elastic isotropic medium are given by

$$\sigma_{ij} = \lambda \varepsilon_{kk} \delta_{ij} + 2\mu \varepsilon_{ij} \tag{2}$$

where λ and μ are Lamé's parameters, δ_{ij} is Kronecker's symbol and ε_{ij} are the strains defined as

$$\varepsilon_{ij} = \frac{1}{2}\left(\frac{\partial u_i}{\partial x_j} + \frac{\partial u_j}{\partial x_i}\right). \tag{3}$$

The material parameters ϱ, λ and μ can be arbitrarily vary in space.

SURFACE TOPOGRAPHY

The surface topography is introduced into the numerical algorithm by mapping a 3-dimensional rectangular grid onto a curved grid. The rectangular grid has a (ξ, v, ζ)-coordinate system, whereas the curved grid has the (x, y, z)-coordinates.

We depart from the following mapping function:

$$x(\xi, v, \zeta) = \xi\,,$$

$$y(\xi, v, \zeta) = v$$

and

$$z(\xi, v, \zeta) = z_0(\xi, v) + \frac{\zeta}{\zeta_{max}}(z_{max} - z_0(\xi, v)) \tag{4}$$

where $z_0(\xi, v)$ is a topography function which describes the elevation above some reference level. z_{max} is the maximum depth of the model which is assumed to have a plane horizontal bottom.

VELOCITY-STRESS FORMULATION ON THE CURVED GRID

We rewrite the equations of motion (1) into a system of first order equations in time (Bayliss et al., 1986; Virieux, 1986) and apply the chain rule to account for the stretching of the grid in the z-direction according to eq.(3):

$$
\begin{aligned}
\varrho\frac{\partial \dot{u}_x}{\partial t} &= \frac{\partial \sigma_{xx}}{\partial \xi} + \frac{\partial \sigma_{xx}}{\partial \zeta}\frac{\partial \zeta}{\partial x} + \frac{\partial \sigma_{xy}}{\partial v} + \frac{\partial \sigma_{xy}}{\partial \zeta}\frac{\partial \zeta}{\partial y} + \frac{\partial \sigma_{xz}}{\partial \zeta}\frac{\partial \zeta}{\partial z} + f_x \\
\varrho\frac{\partial \dot{u}_y}{\partial t} &= \frac{\partial \sigma_{xy}}{\partial \xi} + \frac{\partial \sigma_{xy}}{\partial \zeta}\frac{\partial \zeta}{\partial x} + \frac{\partial \sigma_{yy}}{\partial v} + \frac{\partial \sigma_{yy}}{\partial \zeta}\frac{\partial \zeta}{\partial y} + \frac{\partial \sigma_{yz}}{\partial \zeta}\frac{\partial \zeta}{\partial z} + f_y \\
\varrho\frac{\partial \dot{u}_z}{\partial t} &= \frac{\partial \sigma_{xz}}{\partial \xi} + \frac{\partial \sigma_{xz}}{\partial \zeta}\frac{\partial \zeta}{\partial x} + \frac{\partial \sigma_{yz}}{\partial v} + \frac{\partial \sigma_{yz}}{\partial \zeta}\frac{\partial \zeta}{\partial y} + \frac{\partial \sigma_{zz}}{\partial \zeta}\frac{\partial \zeta}{\partial z} + f_z \\
\frac{\partial \sigma_{xx}}{\partial t} &= \lambda\left(\frac{\partial \dot{u}_x}{\partial \xi} + \frac{\partial \dot{u}_x}{\partial \zeta}\frac{\partial \zeta}{\partial x} + \frac{\partial \dot{u}_y}{\partial v} + \frac{\partial \dot{u}_y}{\partial \zeta}\frac{\partial \zeta}{\partial y} + \frac{\partial \dot{u}_z}{\partial \zeta}\frac{\partial \zeta}{\partial z}\right) + 2\mu\left(\frac{\partial \dot{u}_x}{\partial \xi} + \frac{\partial \dot{u}_x}{\partial \zeta}\frac{\partial \zeta}{\partial x}\right) \\
\frac{\partial \sigma_{yy}}{\partial t} &= \lambda\left(\frac{\partial \dot{u}_x}{\partial \xi} + \frac{\partial \dot{u}_x}{\partial \zeta}\frac{\partial \zeta}{\partial x} + \frac{\partial \dot{u}_y}{\partial v} + \frac{\partial \dot{u}_y}{\partial \zeta}\frac{\partial \zeta}{\partial y} + \frac{\partial \dot{u}_z}{\partial \zeta}\frac{\partial \zeta}{\partial z}\right) + 2\mu\left(\frac{\partial \dot{u}_y}{\partial v} + \frac{\partial \dot{u}_y}{\partial \zeta}\frac{\partial \zeta}{\partial y}\right) \qquad (5) \\
\frac{\partial \sigma_{zz}}{\partial t} &= \lambda\left(\frac{\partial \dot{u}_x}{\partial \xi} + \frac{\partial \dot{u}_x}{\partial \zeta}\frac{\partial \zeta}{\partial x} + \frac{\partial \dot{u}_y}{\partial v} + \frac{\partial \dot{u}_y}{\partial \zeta}\frac{\partial \zeta}{\partial y} + \frac{\partial \dot{u}_z}{\partial \zeta}\frac{\partial \zeta}{\partial z}\right) + 2\mu\left(\frac{\partial \dot{u}_z}{\partial \zeta}\frac{\partial \zeta}{\partial z}\right) \\
\frac{\partial \sigma_{xy}}{\partial t} &= \mu\left(\frac{\partial \dot{u}_x}{\partial v} + \frac{\partial \dot{u}_x}{\partial \zeta}\frac{\partial \zeta}{\partial y} + \frac{\partial \dot{u}_y}{\partial \xi} + \frac{\partial \dot{u}_y}{\partial \zeta}\frac{\partial \zeta}{\partial x}\right) \\
\frac{\partial \sigma_{xz}}{\partial t} &= \mu\left(\frac{\partial \dot{u}_x}{\partial \zeta}\frac{\partial \zeta}{\partial z} + \frac{\partial \dot{u}_z}{\partial \xi} + \frac{\partial \dot{u}_z}{\partial \zeta}\frac{\partial \zeta}{\partial x}\right) \\
\frac{\partial \sigma_{yz}}{\partial t} &= \mu\left(\frac{\partial \dot{u}_y}{\partial \zeta}\frac{\partial \zeta}{\partial z} + \frac{\partial \dot{u}_z}{\partial v} + \frac{\partial \dot{u}_z}{\partial \zeta}\frac{\partial \zeta}{\partial y}\right)
\end{aligned}
$$

A similar approach has been used by Fornberg (1988) to represent curved interfaces in 2-dimensional modeling. For the computation of eq.(5) we need $\frac{\partial \zeta}{\partial x}$, $\frac{\partial \zeta}{\partial y}$ and $\frac{\partial \zeta}{\partial z}$ given by:

$$
\begin{aligned}
\frac{\partial \zeta}{\partial x} &= -\frac{\partial z}{\partial \xi}\left(\frac{\zeta_{max} - \zeta}{z_{max} - z_0}\right) \\
\frac{\partial \zeta}{\partial y} &= -\frac{\partial z}{\partial v}\left(\frac{\zeta_{max} - \zeta}{z_{max} - z_0}\right) , \qquad (6) \\
\frac{\partial \zeta}{\partial z} &= \frac{\zeta_{max}}{z_{max} - z_0}
\end{aligned}
$$

MODELING ALGORITHM

The variables of eq.(5) are discretized on a spatial grid, where the grid spacings in the ξ- and v-directions are uniform and nonuniform in the ζ-direction.

Differencing with respect to the horizontal directions are carried out by the Fourier method, while the vertical derivatives are performed by a Chebyshev derivative operator (Kosloff et al., 1990).

For the time integration a fourth order Taylor expansion of the formal solution in conjunction with time stepping is used (Tessmer, 1991).

FREE SURFACE WITH TOPOGRAPHY

The boundary conditions at a curved free surface are zero normal tractions, i.e. in a local coordinate system with the z'-axis normal to the surface element

$$\sigma'_{xz} = \sigma'_{yz} = \sigma'_{zz} = 0 . \qquad (7)$$

Requiring the above boundary conditions implies modifications of the remaining variables by characteristic treatment (Gottlieb et al., 1982; Bayliss et al., 1986). The modified variables then read (Tessmer et al., 1990):

$$
\begin{aligned}
\sigma'^{\,N}_{yy} &= \sigma'_{yy} - \frac{\lambda}{\lambda + 2\mu}\sigma'_{zz} \\
\sigma'^{\,N}_{xx} &= \sigma'_{xx} - \frac{\lambda}{\lambda + 2\mu}\sigma'_{zz} \\
\dot{u}'^{\,N}_{y} &= \dot{u}'_y + \frac{\sigma'_{yz}}{\sqrt{\varrho\mu}} \qquad (8) \\
\dot{u}'^{\,N}_{x} &= \dot{u}'_x + \frac{\sigma'_{xz}}{\sqrt{\varrho\mu}} \\
\dot{u}'^{\,N}_{z} &= \dot{u}'_z + \frac{\sigma'_{zz}}{\sqrt{\varrho(\lambda + 2\mu)}}
\end{aligned}
$$

The supersprict ^{N} denotes the variables at the free surface after the corrections. Only σ'_{xy} remains unchanged.

Before the application of the characteristic treatment the particle velocities and the stresses which are given in the (x, y, z)-coordinate system must be transformed into the local (x', y', z')-coordinate system where the z'-axis is normal on the surface. The transformation into the local (x', y', z')-coordinate system is given by:

$$
\begin{aligned}
\dot{u}'_i &= a_{ij}\dot{u}_j \\
\sigma'_{ij} &= a_{ik}a_{jl}\sigma_{kl} \qquad (9)
\end{aligned}
$$

with $i, j, k, l = 1, 2, 3$, where a_{ij} are the components of a rotation matrix, and the indices 1,2 and 3 correspond to the x-,y- and z- coordinate, respectively.

The elements of the rotation matrix are given by:

$$
\begin{aligned}
a_{11} &= \cos\vartheta + \alpha^2(1 - \cos\vartheta) \\
a_{12} &= \gamma\sin\vartheta + \alpha\beta(1 - \cos\vartheta) \\
a_{13} &= -\beta\sin\vartheta + \alpha\gamma(1 - \cos\vartheta) \\
a_{21} &= -\gamma\sin\vartheta + \alpha\beta(1 - \cos\vartheta) \\
a_{22} &= \cos\vartheta + \beta^2(1 - \cos\vartheta) \qquad (10) \\
a_{23} &= \alpha\sin\vartheta + \beta\gamma(1 - \cos\vartheta) \\
a_{31} &= \beta\sin\vartheta + \alpha\gamma(1 - \cos\vartheta) \\
a_{32} &= -\alpha\sin\vartheta + \beta\gamma(1 - \cos\vartheta) \\
a_{33} &= \cos\vartheta + \gamma^2(1 - \cos\vartheta)
\end{aligned}
$$

where

$$cos\ \vartheta = \frac{\mathbf{n} \cdot \mathbf{e}_z}{|\mathbf{n}|}$$

$\alpha = \frac{\mathbf{g} \cdot \mathbf{e}_x}{|\mathbf{g}|}$, $\beta = \frac{\mathbf{g} \cdot \mathbf{e}_y}{|\mathbf{g}|}$ and $\gamma = \frac{\mathbf{g} \cdot \mathbf{e}_z}{|\mathbf{g}|}$ and $\mathbf{g} = \mathbf{n} \times \mathbf{e}_z$. The normal vector on the surface element is given by:

$$\mathbf{n} = \left(\frac{\partial z}{\partial x}, \frac{\partial z}{\partial y}, -1 \right)^T .$$

$\mathbf{e}_x, \mathbf{e}_y$ and $\mathbf{e}_z$ are unit vectors.

After the modifications the variables must be transformed back into the original (x, y, z)-coordinate system.

EXAMPLE

The trench model is given in Fig.1. The model is made up of 125 × 125 × 65 grid points in the x-, y- and z-direction, respectively. The gridspacing is 10 m in the center of the grid. The model dimensions are 1250 m × 1250 m × 570 m. However, towards the free surface and the bottom of the model the spacings with respect to the vertical direction are smaller.

The respective seismic velocities for the P- and S-waves are 2000 m/s and 1155 m/s. A vertical point force is applied 10 grid points (52 m) below the surface. The cutoff frequency is 35 Hz with a Ricker like time history. The total propagation time is 800 ms with timesteps of 1 ms. The model has a trench at the surface along the y-direction (Fig.1). The depth of the trench is 28.5 m, i.e. approx. $\frac{1}{4}$ dominant wavelength.

At two receiver lines, parallel and perpendicular to the trench, seismograms were recorded (Fig.2). The seismogram section (vertical component) in the x-direction (Line 1) shows the direct P-wave and with strong amplitude the Rayleigh wave (R). Due to scrattering at the trench the amplitude of the Rayleigh wave is reduced in the right hand part of the sections. Some energy is scattered back to the left hand side (RR). The section in the y-direction (Line 2) shows undisturbed P- and Rayleigh waves. In addition in front of the ordinary Rayleigh wave a secondary Rayleigh wave (PR) induced by scattering of the direct P-wave traveling can be observed.

Snapshots of the wave field of horizontal (xy) and vertical (xz and yz) planes at the propagation times 400 ms and 700 ms are displayed in Fig.3. The xy-snapshots represent the wave field at the surface. The xz- and yz- planes contain receiver line 1 and line 2, respectively, and the source location. The direct P- and S-waves, the head wave (H) and Rayleigh waves (R and RR) are marked in the figure.

CONCLUSION

A spectral method which can handle 3D surface topography with high accuracy has been presented. The incorporation of the boundary conditions has been done in a similar manner as in Tessmer et al. (1990). However the algorithm had to be modified slightly since the normal direction on the surface varies in case of surface topography. The method is allmost of the same efficiency as the algorithm mentioned above. The presented method allows to study near surface effects of wave propagation phenomena which are caused by a rough surface, as there are diffractions, scattering, multiple reflections and converted waves.

ACKNOWLEDGEMENTS

This work has been funded in part by the Commission of the European Communities in the framework of the Joule programme (JOUF 0033), sub-programme Energy from Fossil Sources, Hydrocarbons, and in part by the German Israeli Foundation (GIF) and the Bundesministerium für Forschung und Technologie (BMFT).

REFERENCES

Bayliss,A., Jordan,K.E., LeMesurier,B.J. and Turkel,E., 1986. A fourth-order accurate finite-difference scheme for the computation of elastic waves: Bull.Seis.Soc. Am., 76, 1115-1132

Fornberg,B., 1988. The pseudospectral method: Accurate representation of interfaces in elastic wave calculations: Geophysics, 53, 625-637

Gottlieb,D., Gunzburger,M and Turkel,E., 1982. On numerical boundary treatment of hyperbolic systems for finite difference and finite element methods: SIAM J.Num.Anal., 19, 671-682

Kosloff,D., Kessler,D., Filho,A.Q., Tessmer,E., Behle,A. and Strahilevitz,R., 1990. Solution of the equations of dynamic elasticity by a Chebyshev spectral method: Geophysics, 55, 734-748

Tessmer,E., Tessmer,G., Kosloff, D., and Behle, A., 1990, 3-D Elastic Modeling by a Chebyshev Spectral Method: 60th annual SEG meeting, San Francisco

Tessmer,E., 1991, Three-Dimensional Elastic Seismic Modeling by a Chebyshev Spectral Method: submitted to Geophysics

Virieux,J., 1986. P-SV wave propagation in heterogeneous media: Velocity-stress finite-difference method: Geophysics, 51, 888-901

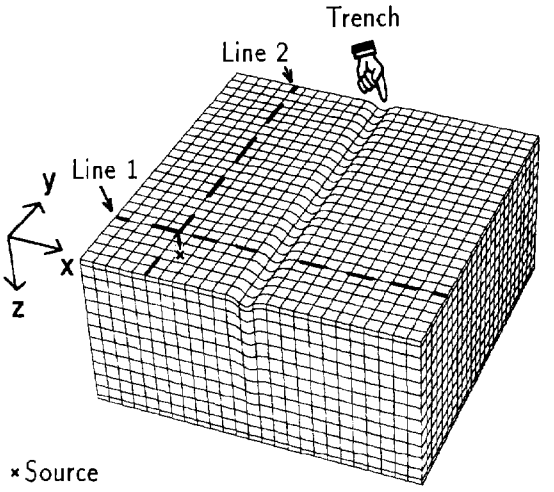

Fig. 1

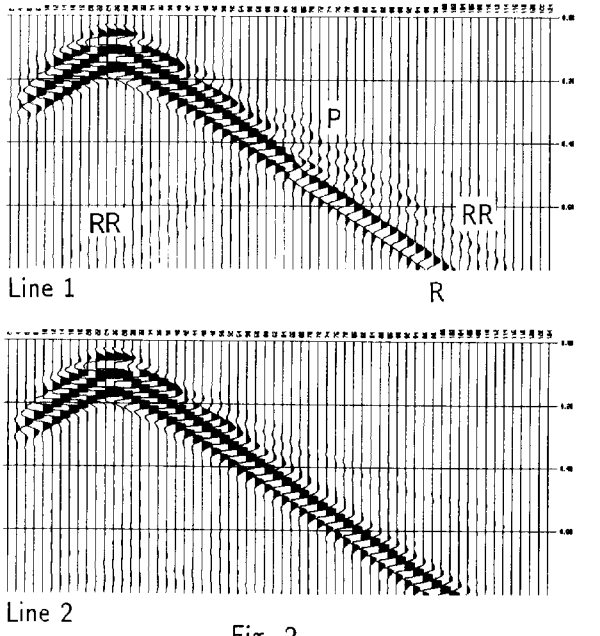

Fig. 2

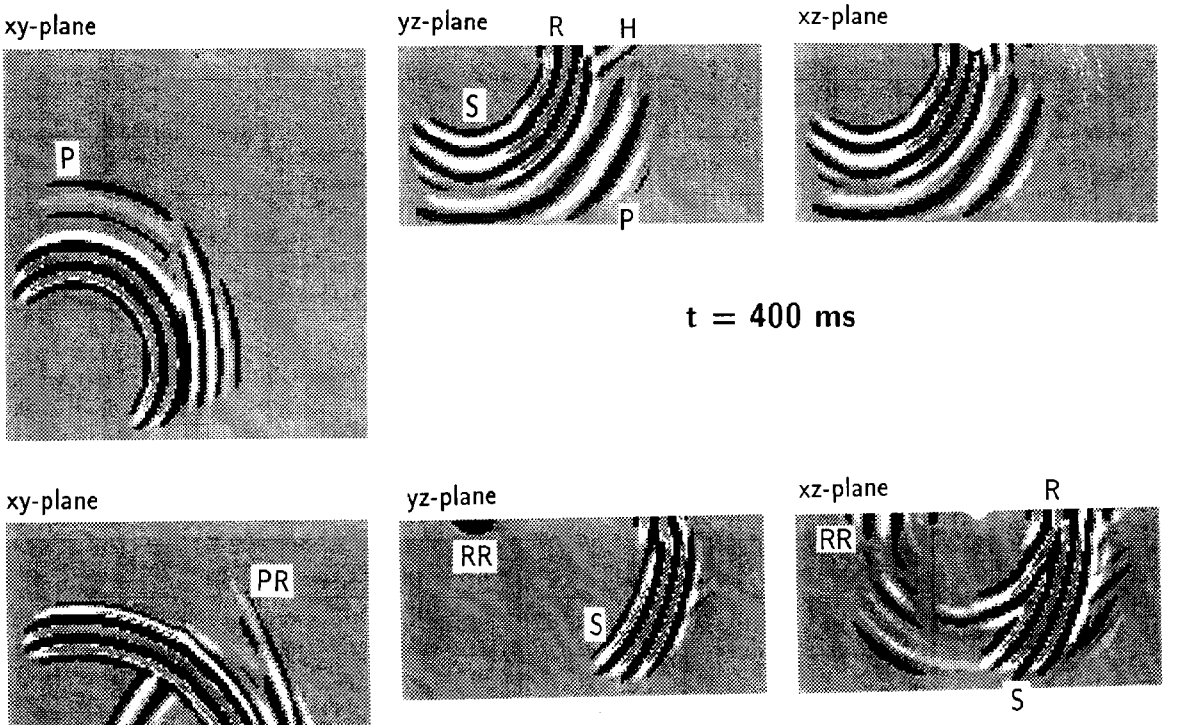

Fig. 3